Netrin-1 controls sympathetic arterial innervation

Isabelle Brunet, … , Holger Eltzschig, Anne Eichmann

Research Article

Autonomic sympathetic nerves innervate peripheral resistance arteries, thereby regulating vascular tone and controlling blood supply to organs. Despite the fundamental importance of blood flow control, how sympathetic arterial innervation develops remains largely unknown. Here, we identified the axon guidance cue netrin-1 as an essential factor required for development of arterial innervation in mice. Netrin-1 was produced by arterial smooth muscle cells (SMCs) at the onset of innervation, and arterial innervation required the interaction of netrin-1 with its receptor, deleted in colorectal cancer (DCC), on sympathetic growth cones. Function-blocking approaches, including cell type–specific deletion of the genes encoding *Ntn1* in SMCs and *Dcc* in sympathetic neurons, led to severe and selective reduction of sympathetic innervation and to defective vasoconstriction in resistance arteries. These findings indicate that netrin-1 and DCC are critical for the control of arterial innervation and blood flow regulation in peripheral organs.

Find the latest version:

https://jci.me/75181/pdf

Netrin-1 controls sympathetic arterial innervation

Isabelle Brunet,[1] Emma Gordon,[2] Jinah Han,[2] Brunella Cristofaro,[1]
Dong Broqueres-You,[3] Chun Liu,[2] Karine Bouvrée,[1] Jiasheng Zhang,[2] Raquel del Toro,[1]
Thomas Mathivet,[1] Bruno Larrivée,[2] Julia Jagu,[1] Laurence Pibouin-Fragner,[1] Luc Pardanaud,[1]
Maria J.C. Machado,[1] Timothy E. Kennedy,[4] Zhen Zhuang,[2] Michael Simons,[2] Bernard I. Levy,[3]
Marc Tessier-Lavigne,[5] Almut Grenz,[6] Holger Eltzschig,[6] and Anne Eichmann[1,2,7]

[1]Centre Interdisciplinaire de Recherche en Biologie (CIRB), Collège de France, Inserm U1050/CNRS UMR7241, Paris, France.
[2]Yale Cardiovascular Research Center, Yale University School of Medicine, New Haven, Connecticut, USA.
[3]Paris Cardiovascular Research Center (PARCC), INSERM U970, Paris, France. [4]Department of Neurology and Neurosurgery,
Montreal Neurological Institute, McGill University, Montreal, Quebec, Canada. [5]Laboratory of Brain Development and Repair,
Rockefeller University, New York, New York, USA. [6]Organ Protection Program, Department of Anesthesiology,
University of Colorado School of Medicine, Anschutz Medical Campus, Aurora, Colorado, USA.
[7]Department of Cellular and Molecular Physiology, Yale University School of Medicine, New Haven, Connecticut, USA.

Autonomic sympathetic nerves innervate peripheral resistance arteries, thereby regulating vascular tone and controlling blood supply to organs. Despite the fundamental importance of blood flow control, how sympathetic arterial innervation develops remains largely unknown. Here, we identified the axon guidance cue netrin-1 as an essential factor required for development of arterial innervation in mice. Netrin-1 was produced by arterial smooth muscle cells (SMCs) at the onset of innervation, and arterial innervation required the interaction of netrin-1 with its receptor, deleted in colorectal cancer (DCC), on sympathetic growth cones. Function-blocking approaches, including cell type–specific deletion of the genes encoding *Ntn1* in SMCs and *Dcc* in sympathetic neurons, led to severe and selective reduction of sympathetic innervation and to defective vasoconstriction in resistance arteries. These findings indicate that netrin-1 and DCC are critical for the control of arterial innervation and blood flow regulation in peripheral organs.

Introduction

Arterial blood vessels and peripheral nerves both form highly branched networks that ramify together throughout the organism (1, 2). To orchestrate the formation of their exquisitely wired networks, nerves and blood vessels have developed specialized cellular guidance structures that respond to common environmental cues (3, 4). Alignment of nerves and blood vessels allows the establishment of a physical relationship between them, notably arterial innervation by autonomic sympathetic nerve fibers that control vascular tone.

Periarterial sympathetic axons surround vessels in lace-like networks. The fibers are confined to the media-adventitia border above the medial smooth muscle cell (SMC) layer and release neurotransmitter from en passant varicosities during conduction of an action potential (5). Maintenance of arterial neurovascular junctions requires vascular endothelial growth factor (6). Innervation density differs between arteries, with large elastic arteries such as the aorta being poorly innervated and small resistance arteries such as the mesenteric and cutaneous arteries showing very dense innervation (7, 8). Sympathetic varicosities induce vasoconstrictor responses in these resistance arteries, thereby reducing peripheral tissue perfusion in environmental stress situations (7, 9). For example, cold stress will activate vasoconstriction of cutaneous arteries and arterioles to reduce skin heat loss and thus to maintain normal core body temperature. Sympathetic regulation of peripheral resistance arteries is essential for maintaining blood flow to the heart and central nervous system under stress conditions (7, 10). Dys-

function of sympathetic arterial innervation contributes to orthostatic hypotension and to essential hypertension (7). Catheter-based renal artery denervation decreases blood pressure in patients with treatment-resistant hypertension (11), indicating that targeting arterial sympathetic innervation offers therapeutic opportunities to develop novel antihypertensive medication.

In addition to blood vessels, sympathetic nerves innervate and control additional targets, including exocrine and endocrine glands, pilomotor muscles, and SMCs of the heart and internal organs (12). Axon projections from sympathetic neurons en route to these targets occur along arterial vasculature (12). For instance, sympathetic neurons of the superior cervical ganglia (SCG) send axonal projections either along the external carotid arteries to innervate the submandibular, sublingual, and parotid glands or along the internal carotid arteries to the lacrimal and pineal glands, the eye, the mucosa of the oral and nasal cavities, and the skin and blood vessels of the head (13). Molecules, such as artemin, neurotrophin-3 (NTF3), and endothelin-3, promote axon extension along arteries, and mouse mutants deficient for these factors exhibit defects in proximal axon extension during midgestation (13–17); however, whether these factors also control arterial innervation per se is unknown.

Arteries are not only paths allowing axons to travel toward end-organ targets, they are themselves targets for innervation. Individual sympathetic axons are therefore presented with the choice of either contacting SMCs of the arterial wall and establishing functional innervation or ignoring these potential targets and, instead, extending along them. We reasoned that two possible mechanisms might regulate this choice: local release of attractants

or repellents from individual SMCs could influence sympathetic growth cone behavior during proximal axon extension or arterial innervation might be temporally controlled and occur after innervation of other sympathetic targets is completed.

Results

To distinguish between these two possibilities, we investigated the onset of arterial innervation by staining with an antibody against tyrosine hydroxylase (TH), the rate-limiting enzyme in catecholamine production in the sympathetic nervous system (18, 19). In E15.5 mouse skin, sympathetic axons selectively extended along Tuj1^{+} sensory axons that were aligned with arteries (ref. 20 and Supplemental Figure 1, A–D; supplemental material available online with this article; doi:10.1172/JCI75181DS1). At P0, whole-mount staining of mesenteric arteries with anti-smooth muscle actin (SMA) and anti-TH antibodies showed that sympathetic axons were present next to arteries, and some larger axon bundles crossed over the artery, but no small fibers extending growth cones toward anti-SMA[+] arterial SMCs were visible (Figure 1, A–D). In P2 mesenteries, sympathetic axons started to extend small-diameter fibers that wrapped around the arterial wall (Figure 1, E–H). High-magnification confocal analysis showed that TH[+] growth cones contacted arterial SMCs at P2 but not at P0 (Figure 1, C, D, G, and H). Double staining with anti-TH and neuron-specific class III β-tubulin Tuj1 antibody or *Wnt1-Cre:mTmG* arteries (21) confirmed that virtually all fibers contacting the arterial wall were TH[+] sympathetic fibers (Supplemental Figure 1, E–P). In P10 mesenteries, arteries were fully surrounded by a lattice of sympathetic axons (Figure 1, I and J), with a density of arterial innervation similar to that seen in adult arteries (see below).

To establish if arterial innervation correlated with maturation of the arterial wall, we used immunostaining of sections of P0, P3, and P10 mesenteries (Figure 1, K–P) and transmission electron microscopy (Figure 1, Q–S). P0 arteries were surrounded by 2 layers of mural cells, but only the inner one was positive for anti-SMA (Figure 1, K, L, and Q). TH[+] nerve fibers were present next to the arteries, but no contacts between individual sympathetic fibers and the arterial wall were visible, confirming results obtained with whole-mount stainings (Figure 1, A, B, K, L, and Q). P3 arteries had developed an internal elastic lamina and acquired a second layer of SMA[+] SMCs around the arterial wall (Figure 1, M and N). Individual TH[+] nerve fibers contacted the second SMC layer and, by electron microscopy, small-diameter nerve fibers were seen to communicate directly with the SMCs in the second layer (Figure 1R). Finally, at P10, the arterial wall was composed of 2 SMC layers surrounded by the external elastic lamina (EEL), and adventitial cells assembling around it (Figure 1, O, P, and S). TH[+] nerve fiber endings contacting SMCs were far more numerous than at P2 (Figure 1, O and P) and communicated with the SMCs through gaps in the EEL (Figure 1S).

To determine whether sympathetic arterial innervation followed a similar time course in other tissues, we performed TH staining of skin and arteries in the Circle of Willis, which showed that, as in the mesentery, sympathetic axons established contacts at P2 and fully surrounded the arterial wall by P10 (Supplemental Figure 1, Q–T).

These observations show that arterial innervation in mice is initiated postnatally (P2) and completed within the second week after birth, concomitant with maturation of the arterial wall (9). In contrast, alignment of sympathetic axons and arteries occurs a week before arterial innervation, and innervation of other sympathetic targets is completed perinatally (17).

We reasoned that the switch from axon elongation along arteries to innervation of arteries might reflect the appearance of an attractive factor(s) generated by arteries. To identify such factors, we screened for transcripts that are differentially expressed in P0 and P2 arteries, using cDNAs isolated from P0 and P2 *Cx40::egfp* mouse arteries. Quantitative PCR (qPCR) showed that transcripts encoding the axon guidance cue netrin-1 (22) were upregulated 1.8-fold in innervated arteries compared with noninnervated arteries (Supplemental Figure 2A). X-gal staining of P0 and P2 mesenteries from heterozygous *Ntn1* knock-in mice (22) showed arterial netrin-1 expression at P2, but not at P0, confirming the qPCR data (Figure 2, A and B).

We also detected netrin-1 expression in arteries of the Circle of Willis at P2 but not at P0 (Figure 2, C–F). During embryonic development, prior to innervation, no netrin-1 was detected, and netrin-1 expression in these arteries persisted until adulthood (Supplemental Figure 2B). Therefore, netrin-1 expression correlates temporally with the onset of arterial innervation.

Netrin-1 expression also correlated spatially with innervated arteries, with high levels in cutaneous arteries (Figure 2G) and in resistance arteries branching off the iliac and femoral artery. No expression was observed in the carotid, aorta, iliac, and femoral arteries (Figure 2, H–J), which are conduit arteries that do not vasoconstrict in response to sympathetic stimulation. Sections of X-gal–stained arteries labeled with anti-SMA showed that netrin-1 was expressed in SMCs surrounding the wall of resistance arteries (Figure 2, K–P).

We asked whether netrin-1 regulates arterial innervation using in vivo function-blocking approaches. As *Ntn1*^{−/−} mice die at birth (22), we generated conditional *Ntn1* mutants by inserting loxP sites around exon 3 of the mouse *Ntn1* gene (Supplemental Figure 2C) and intercrossed *Ntn1*^{fl/fl} mice with *Sm22-Cre* drivers (23) to produce *Sm22-Cre*[+] *Ntn1*^{fl/fl} mice (hereafter referred to as *Ntn1*[smko]). *Ntn1* levels in P3 *Ntn1*[smko] mice were around 50% of those of *Cre*[−] littermate controls (Supplemental Figure 2D). Intercross with *mT:mG* reporter mice (21) confirmed Cre activity in only a subset of arterial SMCs (Supplemental Figure 2E). Nevertheless, quantification of the area of TH[+] axons covering the SMA[+] arterial wall at P3 showed significant reduction of arterial innervation in *Ntn1*[smko] mice compared with *Cre*[−] littermates, despite residual netrin-1 expression (Figure 3, A–C). Furthermore, mesenteries from heterozygous *Ntn1-lacZ* knock-in mice, which expressed half of the wild-type *Ntn1* levels in arterial SMCs (Supplemental Figure 2F), also showed significant reduction of arterial innervation compared with that of wild-type littermates (Figure 3C). Thus, reduction of netrin-1 levels by only 50% significantly reduces arterial innervation. To test effects of temporal blockade of netrin-1, we used intraperitoneal injection of netrin-1 function-blocking antibodies (24) at P1 and P2, followed by quantification of the area of TH[+] nerve fibers covering the mesenteric arteries at P3. Anti–netrin-1–treated mice showed a significant reduction in arterial innervation, like *Ntn1*[smko] and *Ntn1*^{+/−} mice (Figure 3C), indicating that blocking netrin-1 function during the postnatal time window when sympathetic innervation occurs is sufficient to impair arterial innervation.

Since reduction of netrin-1 levels or blocking of netrin-1 function reduced arterial innervation, we asked whether overexpression of netrin-1 could promote sympathetic axon extension in vivo. We injected lentivirally transduced netrin-1–overexpressing pancreatic tumor cells, which secrete 150 ng/ml netrin-1 per
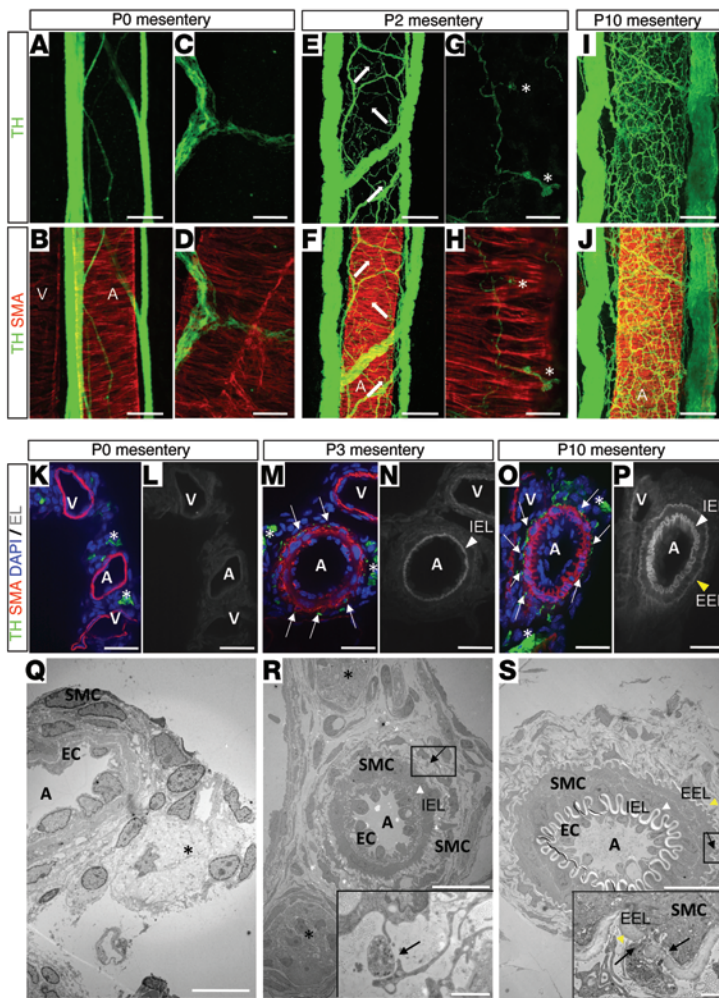
Figure 1
Sympathetic arterial innervation in mice occurs after birth. (**A–J**) Confocal microscopy of mesenteric arteries stained with anti-SMA and anti-TH antibodies. (**A** and **B**) Note no arterial innervation at P0, (**E** and **F**) beginning of innervation at P2 (arrows), and (**I** and **J**) full innervation at P10. High-magnification images show (**C** and **D**) axon bundles crossing over the artery at P0 but absence of individual fibers, (**G** and **H**) whereas single sympathetic fiber growth cones contact the artery wall at P2 (asterisks). (**K–P**) Cryostat section of mesenteric arteries at P0, P3, and P10 stained with indicated markers. Elastin staining showed arterial maturation, (**N**) with internal elastic lamina (IEL, white arrowheads) present at P3 (**L**) but not at P0, and (**P**) the EEL (yellow arrowheads) forming at P10. SMA immunostaining shows 1 layer of SMCs at P0, and 2 layers at P3 and P10. (**M**) TH+ sympathetic fibers start contacting arteries at P3 (arrows), and (**O**) their density increased by P10 (arrows). (**K**, **M**, and **O**) Sympathetic nerve bundles aligned with arteries were visible at P0, P3, and P10 (asterisks). (**Q–S**) Scanning electronic microscopy of mesenteric arteries at P0, P3, and P10. Nerve bundles (asterisks) are present at P0 and P3. Boxes show (**R**) a P3 sympathetic axon contacting SMC extensions and (**S**) a P10 axon contacting a SMC through the EEL. A, artery; EC, endothelial cell. Scale bars: 50 μm (**A**, **B**, **E**, **F**, **I**, and **J**); 10 μm (**C**, **D**, **G**, **H**, and **Q**); 25 μm (**K–P**); 20 μm (**R** and **S**); 1 μm (inset in **R** and **S**).

day (25), intraperitoneally into neonates, thereby flooding the peritoneal cavity with ectopic netrin-1. We reasoned that ectopic overexpression of netrin-1 in the peritoneal cavity should compete with arterial netrin-1 and might attract axons away from the arterial wall. Examination of mesenteric arteries at P8 showed that mice injected with netrin-1–expressing tumor cells exhibited significant deviation of TH+ axons away from the arterial wall, compared with mice injected with control neomycin-expressing tumor cells, which had little or no ectopic sympathetic axons that were not aligned with or surrounding arteries (Figure 3, D and E). Effects of ectopic netrin-1 expression on sympathetic axons could be blocked by coinjection of an antibody that blocks netrin-1 binding to its receptor deleted in colorectal cancer (DCC) (26, 27), but not to UNC5B (ref. 28, Figure 3, D and E, and Supplemental Figure 2G), which led to reduction in ectopic axon extension away from the arterial wall.

These results suggested that netrin-1 might attract sympathetic axons via DCC. Expression of DCC was readily detected in sympathetic axons surrounding mesenteric arteries in vivo and sympathetic growth cones in vitro (Figure 4A). To test whether DCC mediated the response of sympathetic axons to arterial netrin-1, we deleted *Dcc* in sympathetic axons using *Dcc*$^{fl/fl}$ mice and *TH-Cre*^{ER} driver lines (29, 30) by 4-hydroxytamoxifen (4-OHT) injection at P1 and P2, followed by analysis of arterial

innervation at P3. 4-OHT–injected *Cre*$^-$ littermates were used as controls (Figure 4, B–D). In an additional set of neonates, we injected DCC function-blocking antibodies (27) at P1 and P2 (Figure 4E). Both DCC function-blocking approaches led to a significant reduction of arterial innervation at P3 (Figure 4, B–E), mimicking the phenotypes seen after loss of netrin-1 function. Taken together, these experiments are consistent with a model whereby netrin-1 produced by SMCs in the early postnatal arterial wall mediates sympathetic arterial innervation by binding to DCC receptors on sympathetic axons.

SMC coating, arterial diameter, and the diameter of the sympathetic nerve bundles lining the arteries were similar among *Ntn1*^{smko}, *Ntn1*$^{+/-}$, and *Dcc*$^{fl/fl}$ *TH-Cre*^{ER} mice, their littermate controls, and mice injected with netrin and DCC blocking antibodies (Supplemental Figure 3, A and B). Cardiac innervation by TH+ fibers was also similar between wild-type and *Ntn1*$^{+/-}$ littermates (Supplemental Figure 3, C and D). Innervation density in other sympathetic end organs, including testis and bladder, was indistinguishable between wild-type and *Ntn1*$^{+/-}$ mice (data not shown). Together, these data indicate that blocking netrin-1/DCC signaling specifically affected arterial innervation but not other aspects of sympathetic nerve or arterial development.

Netrin-1 binding to DCC mediates axon attraction and branching (31–35), suggesting that netrin-1 might promote arterial
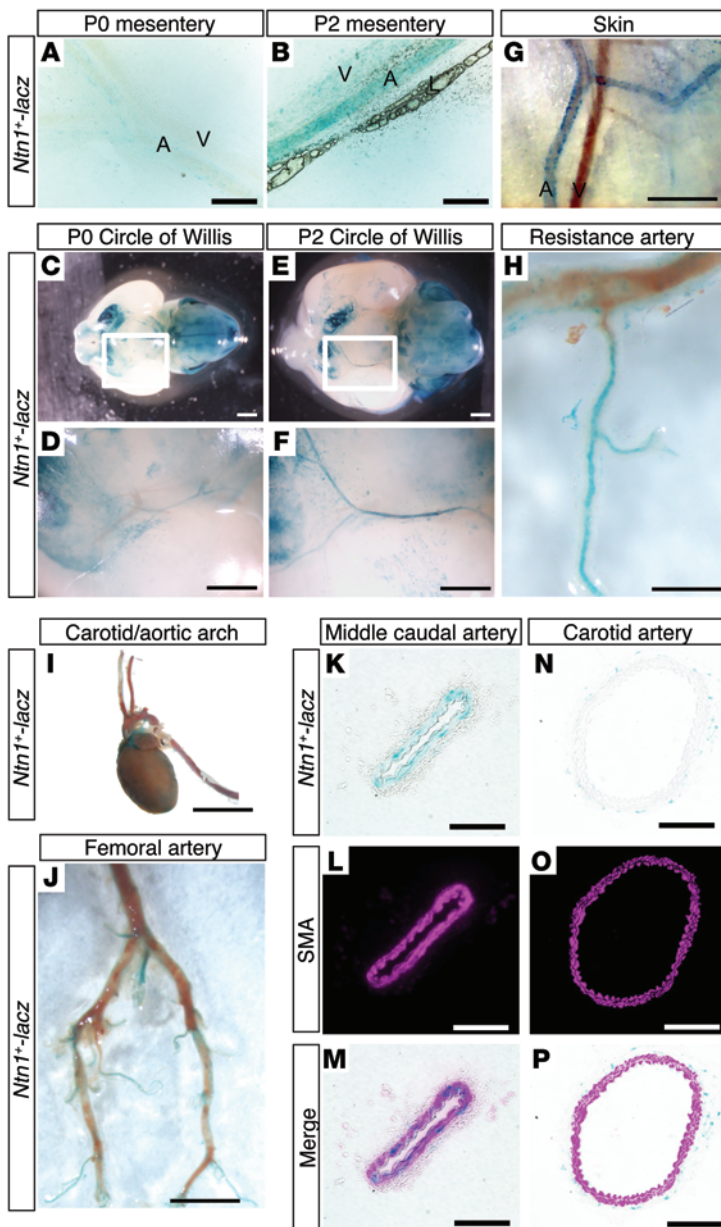
Figure 2
Arterial innervation correlates with netrin-1 expression. X-gal staining of *Ntn1*$^{+/-}$ tissues. (**A**) Note absence of blue netrin-1 staining in noninnervated P0 mesenteric arteries and (**B**) netrin-1 expression at P2 coincident with the onset of arterial innervation. (**C–F**) Arteries in the Circle of Willis start expressing netrin-1 at P2. Images in **D** and **F** show higher-magnification views of the boxed areas in **C** and **E**, respectively. (**G**) Adult skin arteries express netrin-1. (**H**) Resistance arteries branching off the femoral artery are netrin-1 positive. (**I**) Absence of netrin-1 expression in cardiac muscle and carotid arteries. (**J**) Iliac and femoral arteries do not express netrin-1. (**K–M**) Cryostat sections through the middle caudal artery show netrin-1 expression in anti-SMA$^+$ SMCs. (**N–P**) Note absence of netrin-1 staining in SMCs of the carotid artery. V, vein. Scale bars: 200 μm (**A**, **B**, and **H**); 1 mm (**D**, **F**, **G**, and **J**); 2 mm (**C**, **E**, and **I**); 50 μm (**K–M**); 25 μm (**N–P**).

effect on axon branching, growth, extension, or survival, as assessed by quantification of these parameters after 2 and 24 hours (data not shown). Netrin-1 is therefore unlikely to mediate arterial innervation through major effects on sympathetic axon branching or growth. To test for attractive effects, we used cocultures between mesenteric arteries from P8 wild-type and *Ntn1*$^{+/-}$ littermates and wild-type SCG. After 7 days of coculture, in the presence of nerve growth factor (NGF) to stimulate axon outgrowth, TH$^+$ axons were attracted toward and wrapped around wild-type arteries, recapitulating arterial innervation seen in vivo (Supplemental Figure 3, E–I). In contrast, the ability of TH$^+$ axons to move toward and wrap around *Ntn1*$^{+/-}$ arteries was significantly reduced (Supplemental Figure 3, G–I). These observations suggest that netrin-1 is likely to promote arterial innervation by attracting sympathetic axons toward the arterial wall via DCC.

Reduction of netrin-1 levels could lead to a permanent arterial innervation defect or to a transient reduction in innervation that could be compensated for later in life by other factors. In adult *Ntn1*^{smko} and in *Ntn1*$^{+/-}$ mice, confocal microscopy of resistance arteries in the skin and the esophagus showed normal arterial patterning and SMC coating and the presence of TH$^+$ fibers next to the arteries (Figure 5, B–F, and Supplemental Figure 4, A–F). However, in contrast to *Cre*$^-$ or wild-type littermates, in which TH$^+$ fibers surrounded the arterial wall (Figure 5, A and D), TH$^+$ fibers failed to contact arteries in *Ntn1*^{smko} and *Ntn1*$^{+/-}$ mice (Figure 5, B, C, E, and F, and Supplemental Figure 4, A–F). Microdissection of the arterial trees from adult mice showed that the plexus of TH$^+$ sympathetic fibers surrounding arteries in wild-type mice increased in density as artery caliber decreased and reached highest density in peripheral resistance arteries (Figure 5, G and H). *Ntn1*$^{+/-}$ mice showed normal density of TH$^+$ fibers in large-diameter arteries, including the iliac and femoral arteries, but near-complete absence of arterial innervation in resistance arteries (Figure 5I). Transmission electron microscopy of adult mesenteric arteries confirmed that sympathetic axon contacts with SMCs and the area of synaptic varicosities in *Ntn1*$^{+/-}$ mesenteric arteries were reduced compared with those in wild-type littermates (Figure 5, J–M). These results show that a decrease in netrin-1 expression levels causes permanent, severe defects in innervation and synaptic varicosity formation of resistance arteries.

In contrast to the resistance vessels described above, arterial innervation in the Circle of Willis was similar between wild-type and *Ntn1*$^{+/-}$ littermates (Figure 5, N and O). Treatment of *Ntn1*$^{+/-}$ mice with a netrin-1 function-blocking antibody also failed to decrease innervation in these arteries (Figure 5P). Taken together, these data show that innervation of peripheral resistance arteries, but not of cerebral arteries, is highly dependent on netrin-1, thus revealing unanticipated complexity in the mechanisms regulating arterial innervation.

The severe sympathetic innervation defect suggested that adult *Ntn1*^{smko} and *Ntn1*$^{+/-}$ mice should exhibit defective vasoconstriction in response to noradrenalin release from sympathetic nerve terminals in the skin. We evaluated paw cutaneous blood flow by laser-Doppler flowmetry in anesthetized

innervation by attracting DCC-expressing sympathetic axons or by stimulating their branching. Netrin-1 addition to medium that promoted growth of cultured sympathetic neurons had no
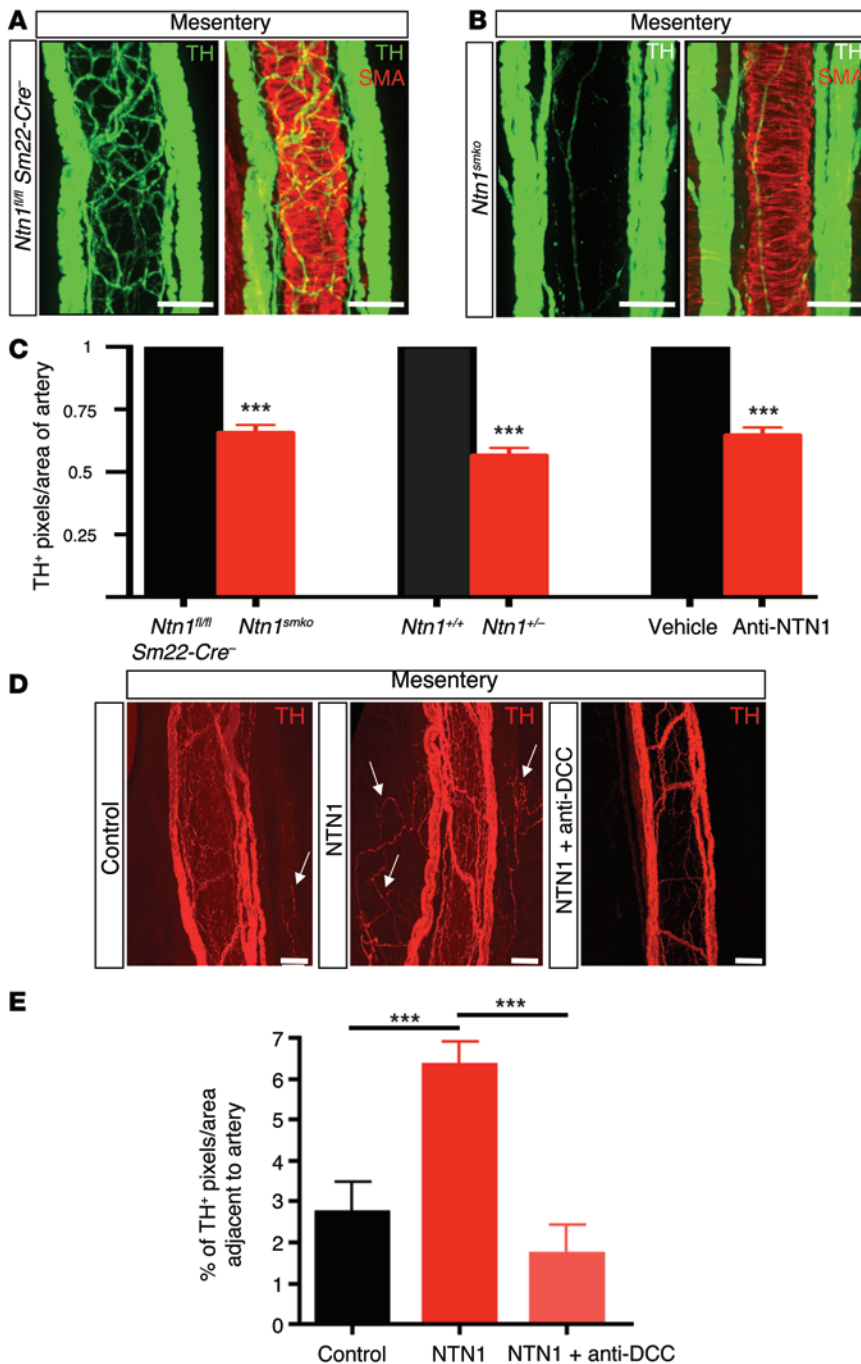
Figure 3
Netrin-1 is required for arterial innervation. (**A** and **B**) Confocal images of mesenteric arteries from (**A**) control and (**B**) *Ntn1smko* mice at P3 stained with anti-TH and anti-SMA antibodies. (**C**) Quantification of mesenteric artery innervation in P3 *Ntn1fl/fl Sm22-Cre⁻* and *Ntn1smko* mice, in wild-type and *Ntn1+/−* mice, and in mice injected with PBS vehicle or an anti–netrin-1 function-blocking antibody (20 μg/g, intraperitoneal injection at P1 and P2). Innervation in control littermates was set as 1. All measurements were made by an observer blinded to the experimental condition ($n = 6$ mice per group, 8–10 images per mesentery). ***$P < 0.0001$, unpaired 2-tailed t test. (**D**) TH immunostaining of mesenteric arteries from P8 mice intraperitoneally injected at P1 with tumor cells transfected with control- or netrin-1–producing expression vector. Note ectopic innervation adjacent to the arteries in mice injected with cells expressing netrin-1, which is abolished when mice were treated with anti-DCC function-blocking antibody (2.5 μg/g, intraperitoneal injection at P2, P5, and P7). (**E**) Ectopic innervation in P8 mice was quantified by measuring the area of TH⁺ pixels adjacent to the arteries. All measurements were made by an observer blinded to the experimental condition ($n = 6$ mice per group, 8 images per mesentery). ***$P < 0.0001$, unpaired 2-tailed t test. Scale bars: 50 μm.

Figure 4, C and D), indicating that SMCs are fully functional in *Ntn1*-deficient mice and that the vasoconstriction defect originates from the presynaptic side.

Discussion

We show that sympathetic arterial innervation in mice occurs within the first 2 weeks after birth, coincident with maturation of the arterial wall. Innervation therefore occurs after alignment of sympathetic axons with arteries and after sympathetic axons have reached other targets in visceral organs (17, 20). Classic studies that traced sympathetic axons projections in rat embryos showed that SCG fibers have reached distal targets as far away as the eye by E15.5, leading the authors to suggest that more proximal end organs, i.e., smooth muscle of the carotid arteries, might receive postganglionic projections even earlier (36). According to this traditional view, the processes of axon extension and innervation may be linked for peripheral arteries. However, the data shown here demonstrate that alignment of sympathetic axons and arterial innervation are temporally uncoupled processes, suggesting that arterial innervation might be triggered by specific signals produced by early postnatal arteries that attract sympathetic axons toward the maturing arterial smooth muscle wall. Future studies are required to determine whether arterial innervation is mediated by branching of sympathetic axons or perhaps by a separate set of
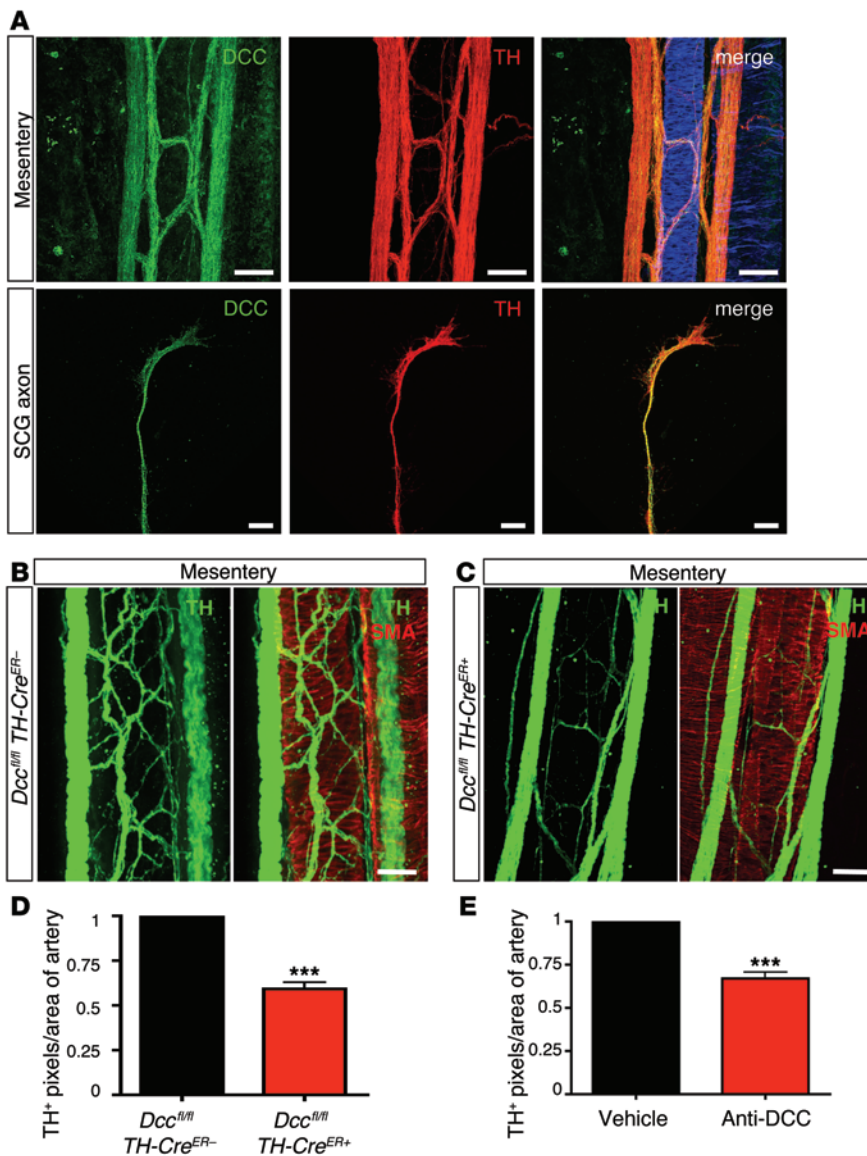
adult mice placed on a temperature-controlled heating pad. In wild-type mice, vasoconstriction was observed when the core body temperature dropped from 38°C to 36°C (Figure 6). In contrast, *Ntn1smko* and *Ntn1+/−* mice exhibited significantly less vasoconstriction in response to the same body temperature decrease (Figure 6). Vasoconstrictor responses in both wild-type and *Ntn1+/−* mice were completely abolished by pretreatment with the α-1 adrenergic receptor blocker prazosin (Figure 6B), indicating that α-1 adrenoreceptors were functional in *Ntn1*-deficient mice. Furthermore, qPCR measurement of adrenoreceptor levels and SMC markers failed to reveal quantitative differences between wild-type and *Ntn1smko* or *Ntn1+/−* arteries (Supplemental

Figure 4
DCC mediates sympathetic innervation in response to netrin-1. (**A**) Anti-DCC immunostaining on TH+ SCG axons in vitro and sympathetic nerves surrounding mesenteric arteries in vivo. (**B** and **C**) Confocal images of P3 mesenteric arteries from *Dcc^fl/fl^TH-Cre* control mice (**B**) and *Dcc^fl/fl^TH-Cre^+^* mice (**C**) injected with 4-OHT at P0, P1, and P2 and stained with anti-TH and anti-SMA antibodies. (**D** and **E**) Quantification of mesenteric artery innervation in *Dcc^fl/fl^TH-Cre* control mice and *Dcc^fl/fl^TH-Cre^+^* mice shown in **B** and **C** and in mice injected with PBS vehicle or an anti-DCC function-blocking antibody (2.5 μg/g, intraperitoneal injection at P1 and P2). Innervation in control littermates was set as 1. All measurements were made by an observer blinded to the experimental condition (*n* = 6 [**E**] and 3 [**D**] mice per group; 8–10 images per mesentery). ***P < 0.0001, unpaired 2-tailed *t* test. Scale bars: 50 μm (**A**, top row, **B**, and **C**); 10 μm (**A**, bottom row).

relates temporally and spatially with arterial innervation. Strikingly, smooth muscle–specific deletion of the *Ntn1* gene, which leads to a 50% reduction in the levels of netrin-1 expression and absence of one copy of the *Ntn1* gene, was sufficient to severely impair arterial innervation in small-diameter resistance arteries branching off the iliac and femoral artery as well as arteries in the skin and internal organs, such as the esophagus and mesentery. Acute temporal netrin-1 blockade during early postnatal life with a function-blocking antibody (37) was sufficient to reduce arterial innervation. Conversely, overexpression of netrin-1 in the peritoneal cavity led to ectopic extension of sympathetic axons away from the arteries, and this process could be blocked by blocking the netrin-1 receptor DCC. Inducible cell type–specific *Dcc* deletion in sympathetic neurons during early postnatal life phenocopied arterial innervation defects seen in *Ntn1*-deficient mice. Together, these data show that netrin-1 produced by postnatal arterial SMCs attracts sympathetic axons via DCC and is required for sympathetic arterial innervation (Figure 7).

DCC expression is detectable in sympathetic axon bundles surrounding mesenteric arteries, but the arterial wall is innervated by a subset of DCC-expressing axons, suggesting that some axons innervate arteries in response to netrin-1/DCC signaling, while others continue to extend. Furthermore, since SMC-specific deletion of *Ntn1* only partially lowered netrin-1 levels and arterial innervation was reduced, but not completely abolished in *Ntn1* mutants, we cannot exclude that other factors may contribute to arterial innervation. Previously identified factors, such as NGF, NTF, and artemin, may participate to this process. Defects in sympathetic outgrowth and alignment with arteries were described in mouse mutants for *Ngf*, *Ntf3*, and the artemin receptor, *Ret*, but perinatal lethality so far precluded analysis of arterial innervation in these mice (38–40). Nevertheless, despite the possible involvement of other factors, partial loss of netrin-1 function was sufficient to induce severe defects in adult artery innervation, functionally leading to loss of vasoconstriction, which was induced

sympathetic neurons. In line with the latter idea, previous studies in the superior cervical ganglion have shown that separate sets of neurons are destined to project axons along the internal or the external carotid artery (13).

Here, we identify the axon guidance cue netrin-1 as the first specific regulator of arterial innervation. We find that netrin-1 is expressed in SMCs of resistance arteries and that its expression cor-

by a drop in core body temperature in anesthetized mice. These data show that even a 50% reduction in netrin-1 levels has functional consequences on blood flow supply to peripheral organs in stress conditions. SMC-specific *Ntn1*-deficient mice therefore present a unique mouse model to study consequences of loss of peripheral arterial sympathetic innervation on blood pressure control and cardiovascular homeostasis in resting and stress conditions.
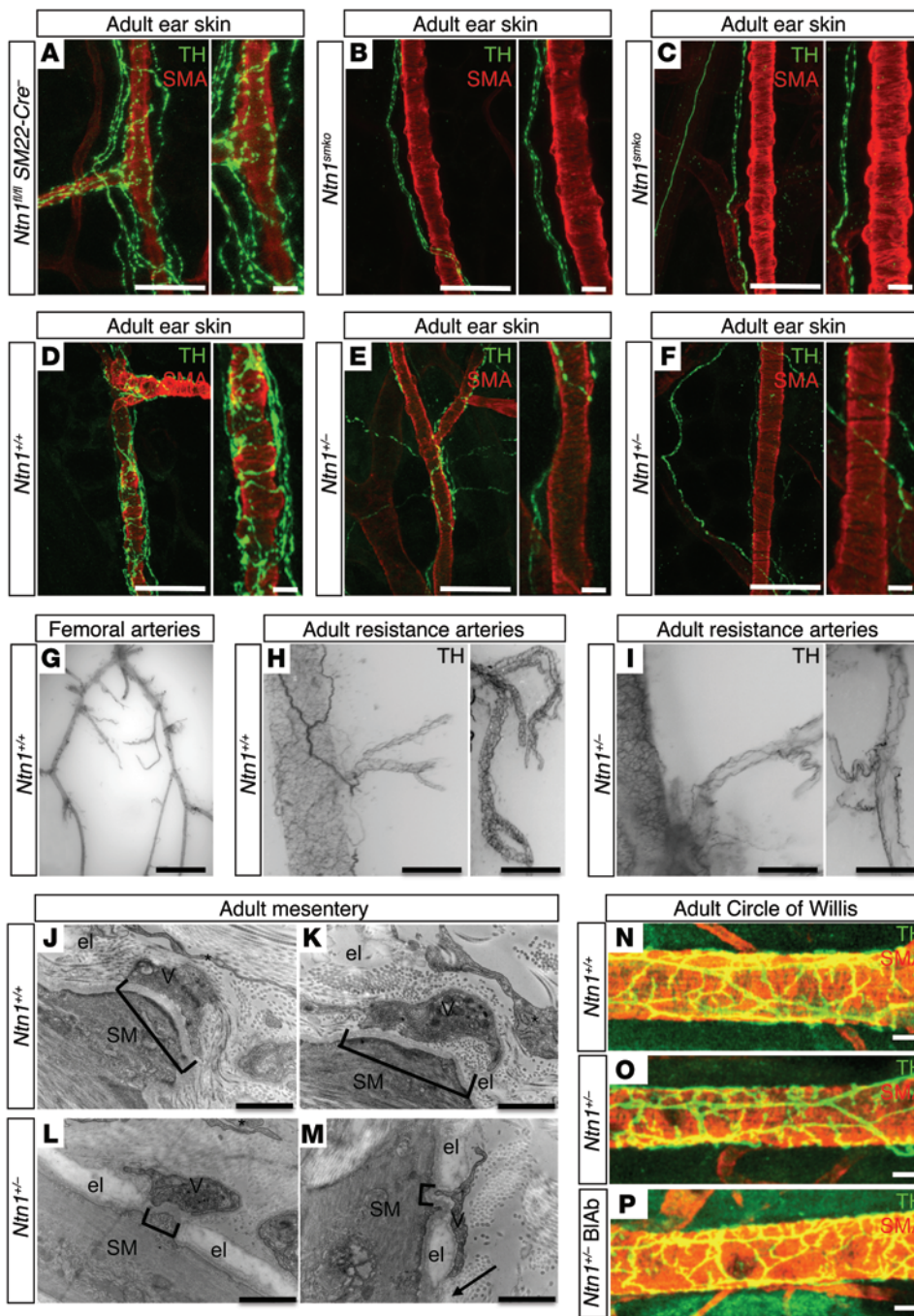
Figure 5
Innervation of peripheral resistance arteries in adult *Ntn1*-deficient mice. (**A–F**) Confocal microscopy shows (**A** and **D**) normal innervation of skin arterioles in *Ntn1*^fl/fl *Sm22-Cre*^– and wild-type mice, while TH^+ fibers are present but fail to contact the arterioles (**B** and **C**) in *Ntn1*^fl/fl *Sm22-Cre*^+ and (**E** and **F**) *Ntn1*^+/– skin. (**G–I**) Anti-TH staining of microdissected iliac and femoral arteries and side branches from adult (**G** and **H**) wild-type and (**I**) *Ntn1*^+/– mice. Images in **H** and **I** were taken of the femoral artery; right panels in **H** and **I** show a higher-magnification images of resistance arteries. (**I**) Note normal femoral artery innervation in *Ntn1*^+/– mice but reduction of resistance artery innervation. (**J–M**) Transmission electron microscopy images from mesenteric arteries of wild-type and *Ntn1*^+/– mice. SM, SMC; el, EEL; V, varicosity. (**N–P**) Similar innervation of arteries in the Circle of Willis in wild-type mice, *Ntn1*^+/– mice, and *Ntn1*^+/– mice treated with an anti–netrin-1 function-blocking antibody (BlAb; 20 μg/g, intraperitoneal injection at P12, P15, and P18; analysis at P20). Scale bars: 50 μm (**A–F**, left panels; **H** and **I**, right panels; and **N–P**); 10 μm (**A–F**, right panels); 100 μm (**H** and **I**, left panels); 1 μm (**J–M**); 2 mm (**G**).

Sympathetic nerves were present and aligned with arteries in *Ntn1*^smko and *Ntn1*^+/– mice, indicating that netrin-1 production by resistance arteries is selectively required for arterial innervation but does not affect development of the sympathetic nervous system per se. Netrin-1 was not expressed in the heart, and cardiac innervation was normal in *Ntn1* mutants. Interestingly, a growing body of evidence indicates that innervation of the heart and large arteries is regulated by other molecules, including NGF and the axon guidance molecule Sema3A and its receptor Nrp1 (41–43). Therefore, sympathetic innervation of cardiovascular targets may be regulated by specific combinations of guidance molecules: Sema3A/Nrp1 for the heart and large arteries and netrin/DCC for resistance arteries.

Innervation of cerebral arteries in the Circle of Willis was also not affected by *Ntn1* deficiency, although these vessels expressed netrin-1. Treatment of *Ntn1*^+/– mice with netrin-1 function-blocking antibody, which reduced mesenteric artery innervation, did not affect innervation of these arteries, indicating that their sympathetic innervation does not depend on netrin-1 but on other, as yet unidentified, cues. Interestingly, sympathetic innervation of these arteries does not contribute significantly to control of cerebral blood flow, which is mainly regulated by neural activity sensed by astrocytes and transmitted to the precapillary arteriole, which dilates to increase blood delivery to the active region (10, 44). These data suggest that netrin-1 is selectively required for sympathetic innervation of peripheral resistance arteries that vasoconstrict in response to sympathetic activation.

In addition to attracting axons toward the arterial wall, netrin-1 may be required for additional steps of arterial innervation, such as the formation of en passant synapses, which starts around P10 and can undergo dynamic changes through adulthood (5). This idea is supported by the observation that defects in arterial innervation in adult resis-
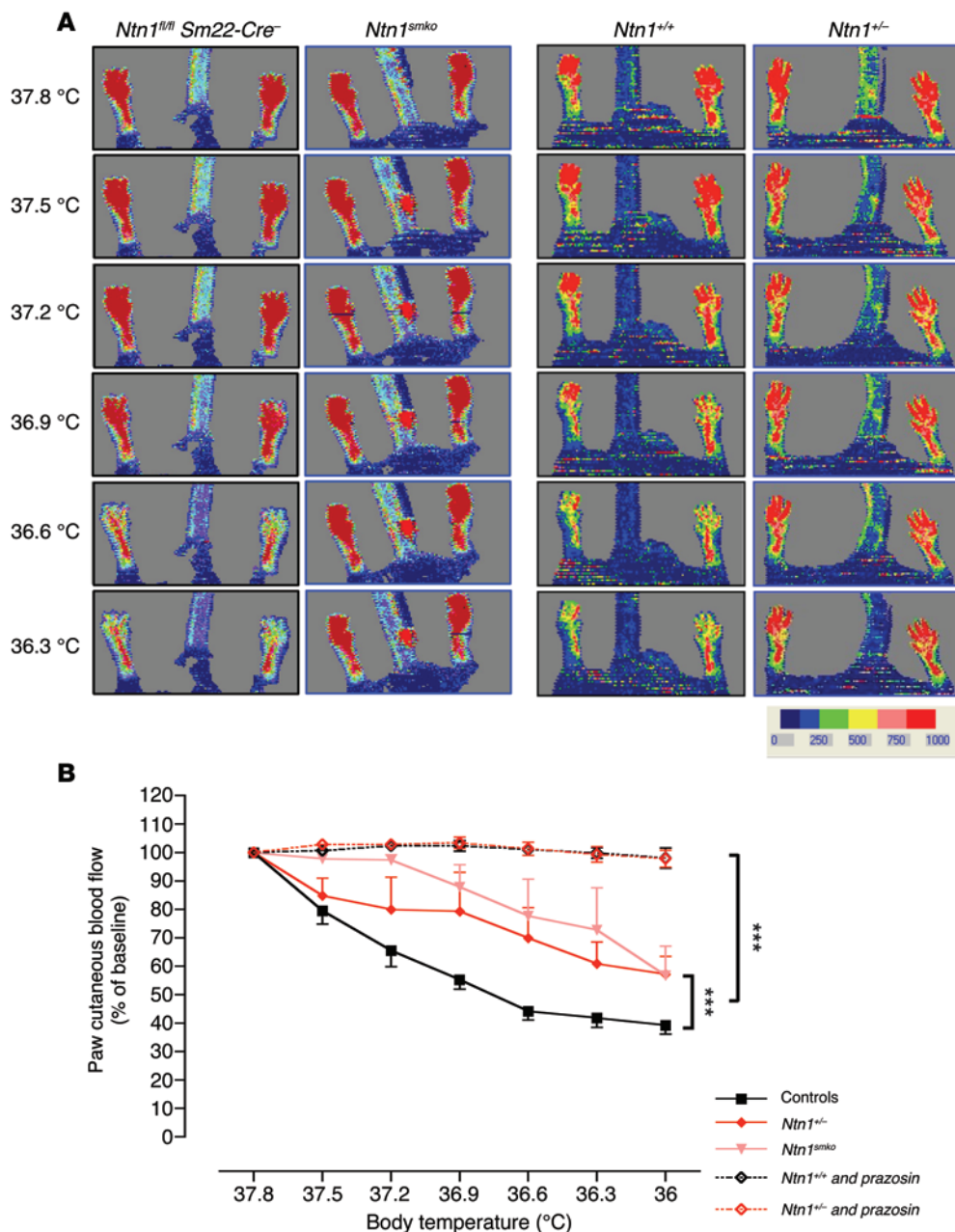
Figure 6
Defective vasoconstriction in *Ntn1^smko^* and *Ntn1^+/–^* mice. (**A**) Laser-Doppler recordings of blood flow in the paws of anesthetized mice monitored for body core temperature. Red color denotes highest blood flow. Note vasoconstriction in *Ntn1^fl/fl^ Sm22-Cre^–^* and in wild-type control mice between 36.9°C and 36.6°C, but absence of vasoconstriction in the *Ntn1^smko^* or *Ntn1^+/–^* littermates ($n = 5$ mice per group for *Ntn1^fl/fl^ Sm22-Cre^–^* and *Cre^+^* and $n = 6$ mice per group for *Ntn1^+/+^* and *Ntn1^+/–^*). (**B**) Laser-Doppler quantification of vasoconstriction in control littermates and *Ntn1^smko^* and *Ntn1^+/–^* mice. At 37.8°C, the foot blood flow was not significantly different between all experimental groups. For each animal, the measurement of foot blood flow at 37.8°C was considered as 100%, and the data of foot blood flow at other temperatures were expressed as the percentages of the measurement at 37.8°C. ***$P < 0.001$, 2-way ANOVA followed by Bonferroni post test. Prazosin treatment (1 mg/kg, intraperitoneal injection 30 minutes prior to the onset of the experiment) abolishes vasoconstriction in both *Ntn1^+/–^* mice and wild-type littermates.

tance arteries are more severe when compared with postnatal arteries and that synaptic area, if it has formed, appears reduced. Netrin-1 plays a role in directing the formation of presynaptic, specialized en passant synapses in *C. elegans* (45, 46), and DCC regulates arborization and synapse formation of dopaminergic axons in the mouse brain (33), suggesting that netrin-1 and DCC may participate in the formation of en passant autonomic synapses.

Besides axon guidance, netrin-1 has been implicated in regulating angiogenesis and arteriogenesis (25, 47–49). Netrin-1 mediates capillary retraction via repulsive UNC5B receptors expressed on endothelial cells and arteriogenesis following hind limb ischemia via an as yet unknown receptor. Netrin-1 also regulates leukocyte-endothelial interactions during inflammation (50–52). As the sympathetic nervous system also regulates production of hematopoietic cells (53), angiogenesis, and arteriogenesis (54, 55), the data

presented here suggest that some of the functions of netrin-1 in blood vessels may be due to its effects on sympathetic axons and underscore the critical role of netrin-1 during coordinated wiring of the nervous and vascular system.

Methods

Animals. Ntn1^+/–^, Cx40-GFP, flk1-GFP, mTmG, Sm22-Cre, TH-Cre, and *Dcc^fl/fl^* mice were described previously (21–23, 29, 30, 56, 57). L. Miquerol (UMR 7288, Marseille, France) provided *Cx40-GFP* mice. *Ntn1^fl/fl^* mice were generated by Ozgene. LoxP sites were inserted on both sides of exon 3 of the mouse *Ntn1* gene, which contained the initiation codons for netrin-1 full-length and short nucleolar forms (58). Cre recombination and exon 3 deletion are predicted to produce a misfolded protein truncated of its 353 N-terminal amino acids, lacking the signal peptide and first 2 laminin EGF-like domains.
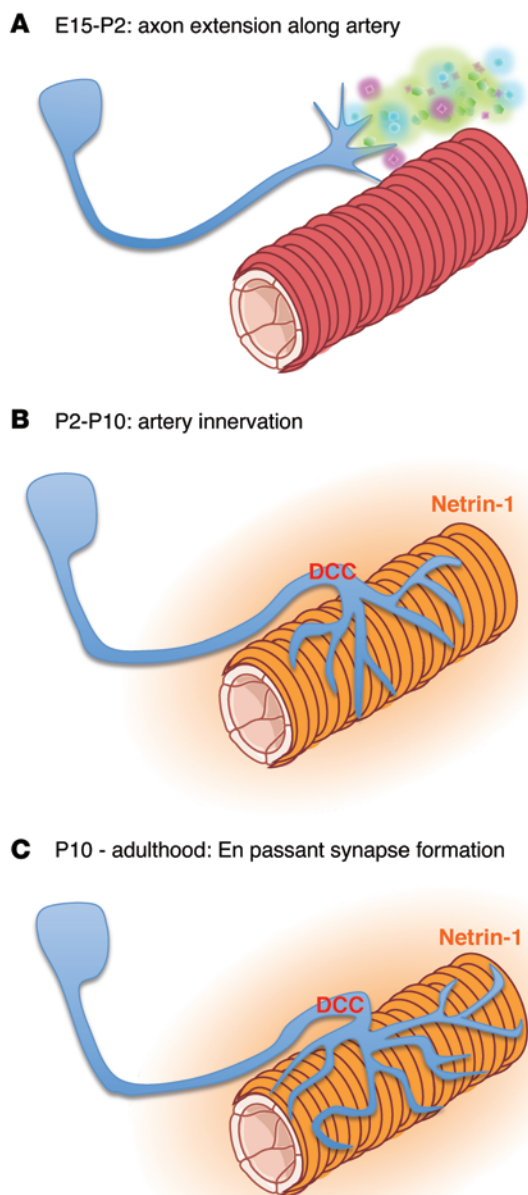
A E15-P2: axon extension along artery

B P2-P10: artery innervation

Netrin-1

DCC

C P10 - adulthood: En passant synapse formation

Netrin-1

DCC

Figure 7
Model for arterial innervation. (**A**) Proximal axon extension along the arterial vasculature occurs before birth and requires molecules, such as endothelins, artemin, and neurotrophins, produced by the arteries (symbolized by colored dots). (**B**) Innervation of arteries occurs at P2, coincident with expression of netrin-1 by SMCs in the arterial wall (symbolized by orange color). (**C**) Full artery innervation and synaptogenesis occurs around P10 and is deficient in small resistance arteries following blocking of netrin-1 and DCC function.

or species-specific fluorescent secondary antibodies (Alexa Fluor 488, 555, or 647; Invitrogen). The samples were then washed in PBS/0.3% Triton X-100 and mounted (Dako Fluorescent Mounting Medium, Dako). Images were captured using a confocal microscope (SP5, Leica) with acquisition software (LAS AF, Leica) and a ×10 NA 0.3 Plan Fluotar lens (HC, Leica), a ×20 NA 0.7 Plan Apo lens (HCX CS, Leica), and a ×40 NA 1.4 Plan Apo lens (HCX CS, Leica). For quantification of mesenteric artery innervation, TH+ area per artery was imaged and analyzed using ImageJ by an observer blinded to the experimental condition.

LacZ staining was performed on 20-μm transverse cryosections of unfixed middle caudal and carotid arteries. After fixation in acetone for 20 minutes at –20°C, slides were washed in washing buffer (0.1% sodium deoxycholate, 0.2% Nonidet P40, and 2 mM $MgCl_2$ in PBS) and incubated overnight at 30°C in X-gal staining solution [2 mM $MgCl_2$, 5 mM $K_4Fe(CN)_6$, 5 mM $K_3Fe(CN)_6$, and 1 mg/ml X-gal in PBS]. Organs were fixed with 4% PFA for 30 minutes at room temperature and then incubated in X-gal staining solution at 30°C for 2 hours or overnight depending on the organ.

Standard procedures were used for transmission electron microscopy.

Cocultures. SCGs from P1 pups were dissected, incubated for 1 hour at 37°C with Mitomycin C (10 mg/ml, Sigma-Aldrich) to arrest nonneural cell growth, and severed into 2 explants. Those explants were placed into type I collagen gel (Rat Tail Collagen, Roche; 100 ml at 3 mg/ml into acetic acid, MEM 10X, $NaHCO_3$) close to mesenteric arteries from P8 wild-type and heterozygous littermates and cultivated in DMEM/F12 medium with 2 mM penicillin/streptomycin, 10% fetal calf serum, 2 mM L-glutamine, and 20 ng/ml NGF (2.5S Nerve Growth Factor, mouse natural, Becton Dickinson) for 7 days at 37°C and 5% CO_2. Collagen gels were fixed with 4% PFA overnight at 4°C and immunostained as described above.

qRT-PCR analysis. Mesenteric arteries from P3 and 6- to 8-week-old $Ntn1^{+/-}$ mice, $Ntn1^{fl/fl}$ $Sm22$-Cre mice, and control littermates were dissected and homogenized. Total RNA was isolated using the RNeasy Mini Kit (Qiagen) according to manufacturer's instructions. The RNA yield was measured by absorbance at 260 nm.

The first-strand cDNA was synthesized by the Bio-Rad iScript cDNA Synthesis Kit. The real-time PCR reactions were performed using IQ SYBR Green Supermix Kit (Bio-Rad) in a CFX96 Real-Time PCR detection system (Bio-Rad). Primers were designed using AlleleID 7 software. The sequences of the primers were as follows: netrin, sense, CTCAGT-GGTTACATACAG, anti-sense, CTCCTCATTTCAGTCTTG; SMA, sense, GGCATCAATCACTTCAAC, anti-sense, CTATCTGGTCACCTGTATG; calponin, sense, AAACAAGAGCGGAGATTTGAGC, anti-sense, TGTC-GCAGTGTTCCATGCC; desmin, sense, CGTGACAACCTGATAGAC, anti-sense, TTCTCTGCTTCTTCTCTTAG; MHC, sense, CAAGATGAT-GAGATGTTC, anti-sense, AAGGACAGATGATACTAC; smoothelin, sense, CCTCAGATACCTTGGACTC, anti-sense, TTGGCAGGATTTCGTTTC; SM22a, sense, CAACAAGGGTCCATCCTACGG, anti-sense, ATCTGGG-CGGCCTACATCA. The β-actin primers were from Qiagen (QT01136772, QuantiTect Primer Assay.) The cycle conditions comprised a 3-minute period of polymerase activation at 95°C and 40 cycles at 95°C for 30 seconds, 30 seconds at 62°C, and 30 seconds at 72°C. Analysis of DNA

Neonatal mouse injections. At day P1, P2 wild-type pups on a CD1 background (*n* = 6 per group) received intraperitoneal injections of 20 μg/g anti–netrin-1 antibody, 2.5 μg/g anti-DCC antibody (Calbiochem), or vehicle PBS. Neonatal pups were collected for analysis at day P3. The $Dcc^{fl/fl}$ TH-Cre^{ER} mice were injected with 100 μg 4-OHT at P0, and tissues were collected at P3. For gain-of-function experiments, pups were injected at P2 with Miapaca cells (1 million cells per intraperitoneal injection) expressing control vector or netrin-1 and injected with blocking antibody anti-DCC at P2, P5, and P7, and then sacrificed at P8.

Immunostaining and histology. For whole-mount staining, dissected tissues were fixed in 4% PFA for 2 hours on ice and blocked overnight in blocking buffer (PBS/0.5% blocking reagent [Perkin]/0.3% Triton X-100/0.2% BSA). Tissues and embryos were incubated overnight at 4°C with primary antibodies in blocking buffer (anti-TH [Millipore, 1:100]; anti-TuJ1 [R&D Systems, 1:100]; and Cy3-conjugated anti-SMA [Sigma-Aldrich, 1:200]). Tissues were washed in PBS/0.3% Triton X-100 and incubated overnight with fluorescent streptavidin (Cy5, GE Healthcare)

melting curves demonstrated a single peak for each set of primers. Amplification products were size controlled on a 1% agarose gel. Quantitative data were normalized relative to the internal housekeeping control β-actin gene. Results are presented as data normalized to the expression of the corresponding gene in control littermate.

One-way ANOVA was used to determine whether there were any significant differences between the gene expression levels in netrin-1–deleted mice and their control littermates.

ELISA. 96-well plates (Maxisorp, Nunc) were coated using 100 µl of 1 µg/ml rmDCC-Fc or rmUNC5B-Fc (R&D Systems) diluted in 1× PBS and incubated overnight at 4°C. Plates were washed 6 times with PBS-Tween (1× PBS; 0.05% Tween20) and blocked by adding 300 µl blocking solution (1× PBS; 0.05% Tween20; 1% BSA) to each well for 1 hour at room temperature. Plates were washed 6 times and incubated with various concentrations of DCC blocking antibody (50, 10, 5, 1, 0.5, 0.1, and 0.05 µg/ml; Calbiochem), 100 µl per well, for 2 hours at room temperature. After 6 washes, plates were incubated with 0.5 µg/ml rmnetrin-1, 100 µl per well, for 2 hours at room temperature. After 6 washes, ELISA detection was performed by incubation with anti–mnetrin-1 biotinylated antibody (0.1 µg/ml; R&D Systems) for 2 hours at room temperature. After 6 washes, ELISA revelation was performed with R&D Systems substrate reagent pack incubated for 10 minutes at room temperature and blocked. Results were obtained by reading sample optical density with a 96-well plate reader (Thermo Scientific) at 450 to 550-nm wavelength.

Laser-Doppler flow. Adult mice were anesthetized using 1.5% isoflurane in air at a flow rate of 1 l per minute. Mice were next placed on a heating platform, and core body temperature was monitored continuously by refined monitoring systems. Using laser-Doppler flowmetry (59), the evaluation of paw cutaneous blood flow was then measured at every 0.3°C drop of body temperature from 37.8°C ± 0.1°C to 35.1°C ± 0.1°C (Moon Instruments). Two weeks later, the same experiment was conducted on those animals treated with an α-1 adrenergic receptor antagonist (1 mg/kg via intraperitoneal injection, prazosin hydrochloride, Sigma-Aldrich) (60).

Statistics. Data shown are expressed as mean ± SEM. The statistical significance was determined using unpaired 2-tailed Student's *t* test. One-way ANOVA was used to determine whether there were any significant differ-ences between the gene expression levels in netrin-1–deleted mice and their control littermates. Statistical analysis for laser-Doppler experiments was performed using 2-way ANOVA followed by Bonferroni post test for group comparison. Statistical analysis was performed using GraphPad Prism software. *P* values of less than 0.05 were considered significant in all experiments.

Study approval. All experimental protocols were approved by Yale University Institutional Animal Care and Use Committee and the CIRB ethical committee and were conducted in accordance with the ARRIVE guidelines for the care and use of laboratory animals.

Address correspondence to: Anne Eichmann, Internal Medicine – Cardiology, PO Box 208017, New Haven, Connecticut 06520-8017, USA. Phone: 203.737.5205; Fax: 203.737.6236; E-mail: anne.eichmann@yale.edu. Or to: Isabelle Brunet, Centre Interdisciplinaire de Recherche en Biologie, CNRS UMR 7241/INSERM U1050, Collège de France, 11, place Marcelin Berthelot, 75231 Paris Cedex 05, France. Phone: 33.1.44.27.16.93; Fax: 33.1.44.27.16.91; E-mail: isabelle.brunet@college-de-france.fr.

1. Carmeliet P, Tessier-Lavigne M. Common mechanisms of nerve and blood vessel wiring. *Nature*. 2005;436(7048):193–200.
2. Adams RH, Eichmann A. Axon guidance molecules in vascular patterning. *Cold Spring Harb Perspect Biol*. 2010;2(5):a001875.
3. Larrivee B, Freitas C, Suchting S, Brunet I, Eichmann A. Guidance of vascular development: lessons from the nervous system. *Circ Res*. 2009;104(4):428–441.
4. Tam SJ, Watts RJ. Connecting vascular and nervous system development: angiogenesis and the blood-brain barrier. *Annu Rev Neurosci*. 2010;33:379–408.
5. Burnstock G. Non-synaptic transmission at autonomic neuroeffector junctions. *Neurochem Int*. 2008;52(1–2):14–25.
6. Storkebaum E, et al. Impaired autonomic regulation of resistance arteries in mice with low vascular endothelial growth factor or upon vascular endothelial growth factor trap delivery. *Circulation*. 2010;122(3):273–281.
7. Storkebaum E, Carmeliet P. Paracrine control of vascular innervation in health and disease. *Acta Physiol (Oxf)*. 2011;203(1):61–86.
8. Luff SE. Ultrastructure of sympathetic axons and their structural relationship with vascular smooth muscle. *Anat Embryol (Berl)*. 1996;193(6):515–531.
9. Luff SE. Development of neuromuscular junctions on small mesenteric arteries of the rat. *J Neurocytol*. 1999;28(1):47–62.
10. Iadecola C, Nedergaard M. Glial regulation of the cerebral microvasculature. *Nat Neurosci*. 2007;10(11):1369–1376.
11. Krum H, et al. Percutaneous renal denervation in patients with treatment-resistant hypertension: final 3-year report of the Symplicity HTN-1 study. *Lancet*. 2014;383(9917):622–629.
12. Glebova NO, Ginty DD. Growth and survival signals controlling sympathetic nervous system development. *Annu Rev Neurosci*. 2005;28:191–222.
13. Makita T, Sucov HM, Gariepy CE, Yanagisawa M, Ginty DD. Endothelins are vascular-derived axonal guidance cues for developing sympathetic neurons. *Nature*. 2008;452(7188):759–763.
14. Enomoto H, Crawford PA, Gorodinsky A, Heuckeroth RO, Johnson EM Jr, Milbrandt J. RET signaling is essential for migration, axonal growth and axon guidance of developing sympathetic neurons. *Development*. 2001;128(20):3963–3974.
15. Honma Y, et al. Artemin is a vascular-derived neurotropic factor for developing sympathetic neurons. *Neuron*. 2002;35(2):267–282.
16. Kuruvilla R, et al. A neurotrophin signaling cascade coordinates sympathetic neuron development through differential control of TrkA trafficking and retrograde signaling. *Cell*. 2004;118(2):243–255.
17. Glebova NO, Ginty DD. Heterogeneous requirement of NGF for sympathetic target innervation in vivo. *J Neurosci*. 2004;24(3):743–751.
18. Zhou QY, Quaife CJ, Palmiter RD. Targeted disruption of the tyrosine hydroxylase gene reveals that catecholamines are required for mouse fetal development. *Nature*. 1995;374(6523):640–643.
19. Flatmark T. Catecholamine biosynthesis and physiological regulation in neuroendocrine cells. *Acta Physiol Scand*. 2000;168(1):1–17.
20. Mukouyama YS, Shin D, Britsch S, Taniguchi M, Anderson DJ. Sensory nerves determine the pattern of arterial differentiation and blood vessel branching in the skin. *Cell*. 2002;109(6):693–705.
21. Muzumdar MD, Tasic B, Miyamichi K, Li L, Luo L. A global double-fluorescent Cre reporter mouse. *Genesis*. 2007;45(9):593–605.
22. Serafini T, et al. Netrin-1 is required for commissural axon guidance in the developing vertebrate nervous system. *Cell*. 1996;87(6):1001–1014.
23. Holtwick R, et al. Smooth muscle-selective deletion of guanylyl cyclase-A prevents the acute but not chronic effects of ANP on blood pressure. *Proc Natl Acad Sci U S A*. 2002;99(10):7142–7147.
24. Metin C, Deleglise D, Serafini T, Kennedy TE, Tessier-Lavigne M. A role for netrin-1 in the guidance of cortical efferents. *Development*. 1997;124(24):5063–5074.
25. Larrivee B, et al. Activation of the UNC5B receptor by Netrin-1 inhibits sprouting angiogenesis. *Genes Dev*. 2007;21(19):2433–2447.
26. Keino-Masu K, et al. Deleted in colorectal cancer (DCC) encodes a netrin receptor. *Cell*. 1996;87(2):175–185.

27. Jarjour AA, Manitt C, Moore SW, Thompson KM, Yuh SJ, Kennedy TE. Netrin-1 is a chemorepellent for oligodendrocyte precursor cells in the embryonic spinal cord. *J Neurosci.* 2003;23(9):3735–3744.

28. Leonardo ED, Hinck L, Masu M, Keino-Masu K, Ackerman SL, Tessier-Lavigne M. Vertebrate homologues of C. elegans UNC-5 are candidate netrin receptors. *Nature.* 1997;386(6627):833–838.

29. Krimpenfort P, Song JY, Proost N, Zevenhoven J, Jonkers J, Berns A. Deleted in colorectal carcinoma suppresses metastasis in p53-deficient mammary tumours. *Nature.* 2012;482(7386):538–541.

30. Rotolo T, Smallwood PM, Williams J, Nathans J. Genetically-directed, cell type-specific sparse labeling for the analysis of neuronal morphology. *PLoS One.* 2008;3(12):e4099.

31. de la Torre JR, et al. Turning of retinal growth cones in a netrin-1 gradient mediated by the netrin receptor DCC. *Neuron.* 1997;19(6):1211–1224.

32. Manitt C, Nikolakopoulou AM, Almario DR, Nguyen SA, Cohen-Cory S. Netrin participates in the development of retinotectal synaptic connectivity by modulating axon arborization and synapse formation in the developing brain. *J Neurosci.* 2009;29(36):11065–11077.

33. Xu B, et al. Critical roles for the netrin receptor deleted in colorectal cancer in dopaminergic neuronal precursor migration, axon guidance, and axon arborization. *Neuroscience.* 2010;169(2):932–949.

34. Goldman JS, et al. Netrin-1 promotes excitatory synaptogenesis between cortical neurons by initiating synapse assembly. *J Neurosci.* 2013;33(44):17278–89.

35. Dent EW, Barnes AM, Tang F, Kalil K. Netrin-1 and semaphorin 3A promote or inhibit cortical axon branching, respectively, by reorganization of the cytoskeleton. *J Neurosci.* 2004;24(12):3002–3012.

36. Rubin E. Development of the rat superior cervical ganglion: ganglion cell maturation. *J Neurosci.* 1985;5(3):673–684.

37. Shekarabi M, Kennedy TE. The netrin-1 receptor DCC promotes filopodia formation and cell spreading by activating Cdc42 and Rac1. *Mol Cell Neurosci.* 2002;19(1):1–17.

38. Crowley C, et al. Mice lacking nerve growth factor display perinatal loss of sensory and sympathetic neurons yet develop basal forebrain cholinergic neurons. *Cell.* 1994;76(6):1001–1011.

39. Ernfors P, Lee KF, Kucera J, Jaenisch R. Lack of neurotrophin-3 leads to deficiencies in the peripheral nervous system and loss of limb proprioceptive afferents. *Cell.* 1994;77(4):503–512.

40. Schuchardt A, D'Agati V, Larsson-Blomberg L, Costantini F, Pachnis V. Defects in the kidney and enteric nervous system of mice lacking the tyrosine kinase receptor Ret. *Nature.* 1994;367(6461):380–383.

41. Nam J, et al. Coronary veins determine the pattern of sympathetic innervation in the developing heart. *Development.* 2013;140(7):1475–1485.

42. Maden CH, Gomes J, Schwarz Q, Davidson K, Tinker A, Ruhrberg C. NRP1 and NRP2 cooperate to regulate gangliogenesis, axon guidance and target innervation in the sympathetic nervous system. *Dev Biol.* 2012;369(2):277–85.

43. Long JB, Jay SM, Segal SS, Madri JA. VEGF-A and Semaphorin3A: modulators of vascular sympathetic innervation. *Dev Biol.* 2009;334(1):119–132.

44. Carmignoto G, Gomez-Gonzalo M. The contribution of astrocyte signalling to neurovascular coupling. *Brain Res Rev.* 2010;63(1–2):138–148.

45. Colón-Ramos DA. Synapse formation in developing neural circuits. *Curr Top Dev Biol.* 2009; 87:53–79.

46. Colon-Ramos DA, Margeta MA, Shen K. Glia promote local synaptogenesis through UNC-6 (netrin) signaling in C. elegans. *Science.* 2007; 318(5847):103–106.

47. Lu X, et al. The netrin receptor UNC5B mediates guidance events controlling morphogenesis of the vascular system. *Nature.* 2004;432(7014):179–186.

48. Wilson BD, et al. Netrins promote developmental and therapeutic angiogenesis. *Science.* 2006;313(5787):640–644.

49. van Gils JM, et al. The neuroimmune guidance cue netrin-1 promotes atherosclerosis by inhibiting the emigration of macrophages from plaques. *Nat Immunol.* 2012;13(2):136–143.

50. Aherne CM, et al. Neuronal guidance molecule netrin-1 attenuates inflammatory cell trafficking during acute experimental colitis. *Gut.* 2012; 61(5):695–705.

51. Ly NP, et al. Netrin-1 inhibits leukocyte migration in vitro and in vivo. *Proc Natl Acad Sci U S A.* 2005; 102(41):14729–14734.

52. Tadagavadi RK, Wang W, Ramesh G. Netrin-1 regulates Th1/Th2/Th17 cytokine production and inflammation through UNC5B receptor and protects kidney against ischemia-reperfusion injury. *J Immunol.* 2010;185(6):3750–3758.

53. Katayama Y, et al. Signals from the sympathetic nervous system regulate hematopoietic stem cell egress from bone marrow. *Cell.* 2006;124(2):407–421.

54. Chalothorn D, Zhang H, Clayton JA, Thomas SA, Faber JE. Catecholamines augment collateral vessel growth and angiogenesis in hindlimb ischemia. *Am J Physiol Heart Circ Physiol.* 2005;289(2):H947–H959.

55. Luo MY, et al. Collateral vessel growth induced by femoral artery ligature is impaired by denervation. *Mol Cell Biochem.* 2011;354(1–2):219–229.

56. Miquerol L, et al. Architectural and functional asymmetry of the His-Purkinje system of the murine heart. *Cardiovasc Res.* 2004;63(1):77–86.

57. Xu Y, et al. Neuropilin-2 mediates VEGF-C-induced lymphatic sprouting together with VEGFR3. *J Cell Biol.* 2010;188(1):115–130.

58. Delloye-Bourgeois C, et al. Nucleolar localization of a netrin-1 isoform enhances tumor cell proliferation. *Sci Signal.* 2012;5(236):ra57.

59. You D, et al. Increase in vascular permeability and vasodilation are critical for proangiogenic effects of stem cell therapy. *Circulation.* 2006;114(4):328–338.

60. Oh-hashi Y, et al. Elevated sympathetic nervous activity in mice deficient in alphaCGRP. *Circ Res.* 2001;89(11):983–990.